

**THE X-RAY CORE OF THE LOW-LUMINOSITY RADIO GALAXY 3C346 and
ASCA SPECTROSCOPY TO TEST BL LAC/RADIO GALAXY UNIFICATION**

NASA Grant NAG5-2961

Final Report

For the Period 15 June 1995 through 31 January 2000

Principal Investigator
Dr. Diana Worrall

June 2000

Prepared for:

National Aeronautics and Space Administration
Goddard Space Flight Center
Greenbelt, Maryland 20771

Smithsonian Institution
Astrophysical Observatory
Cambridge, Massachusetts 02138

<p>The Smithsonian Astrophysical Observatory is a member of the Harvard-Smithsonian Center for Astrophysics</p>

The NASA Technical Officer for this grant is Dr. Nicholas White, Code 668, Laboratory for High Energy Astrophysics, NASA/Goddard Space Flight Center, Greenbelt, Maryland 20771.

Radio galaxies are relatively faint sources for ASCA, and so in order to get the best possible results from the observations two things have been necessary, both of which delayed the fast preparation of papers. Firstly, the best possible data screening and background subtraction were necessary to improve the signal-to-noise, and all our several initial analysis trials were discarded in favor of using FTOOLS versions 4.1 and above. Secondly, we found that the ASCA spectra were statistically too poor to discriminate well between non-thermal and thermal models, never mind the mixture of the two which we expected on the basis of our ROSAT spatial separation of components in radio galaxies. This means that in each case we have needed to combine the ASCA spectroscopy with analysis of data from other X-ray or radio observations in order to exploit the ASCA data to the full.

Our analysis for 3C 346 has yielded the cleanest final result. This powerful radio galaxy, at a redshift of 0.161, lies in a poor cluster, which we have separated well from the dominant X-ray component of unresolved emission using a spatial analysis of archival ROSAT data. We were then able to fix the thermal component in our ASCA spectral analysis, and have found evidence that the unresolved emission varied by $32 \pm 13\%$ over the 18 months between the ROSAT and ASCA observations. The unresolved X-ray emission does not suffer from intrinsic absorption, and we have related it to radio structures on both milliarcsecond scales and the arcsecond scales which *Chandra* can resolve. The source is a target of a *Chandra* AO2 proposal which we have recently submitted to follow up on our ASCA (and ROSAT) work. 3C 346's orientation to the line of sight is uncertain. However, the absence of X-ray absorption, and the radio/optical/X-ray colors, when combined with previous radio evidence that the source is a foreshortened radio galaxy of the FR II class, suggest that the radio jets are seen at an angle to the line of sight of about 30° , intermediate between the radio-galaxy and quasar classes. The relatively hard ASCA response has allowed us to place an upper limit of 5.6×10^{43} ergs s⁻¹ on the 2-10 keV luminosity of any central X-ray component absorbed by gas which might be obscuring the broad-line emission region. Attached to this report is an almost final draft of a paper which we have prepared for submission to the *Astrophysical Journal*.

Our combined ASCA and ROSAT results for NGC 6251 rule out our previously preferred flat-spectrum model and inverse-Compton interpretation for the source based on ROSAT data alone (Birkinshaw & Worrall 1993, ApJ, 412, 568), but a softer X-ray spectrum and moderate absorption bring all the available data (including our early VLA HI measurements) into consistency, and we are reasonably confident that we understand the processes responsible for the X-ray emission. We have made some more sensitive HI absorption measurements which are currently being analyzed, and our plans are to publish our ASCA analysis in conjunction with the new HI results.

The ASCA data for NGC 4261 have been difficult to interpret. A re-analysis of our ROSAT data with a wider range of physical parameters brings the ROSAT and ASCA results into reasonable agreement only if the emission from hot gas dominates more than suggested by our earlier work (Worrall & Birkinshaw 1994, 427, 134), which is itself unexpected since the radio core is bright and a large jet-related X-ray component would bring the source into agreement with results for others of its type. However, we have recently received our

Chandra AO1 data for this source, with the spatial resolution which allows us to separate thermal and non-thermal emission components. Our ASCA results will be re-interpreted once the analysis of our *Chandra* data is complete. The interpretation of the ASCA data for BL Lac object 3C 371 is ongoing, in conjunction with analysis of archival multifrequency data.

Radio galaxies are complex in their X-ray properties, and hindsight has shown that the spatial resolution of ASCA is too poor for a reliable interpretation of the data without drawing on other observations. However, the ASCA spectra have made a useful contribution to the interpretation of these sources, and the groundwork is now there for more sensitive work using *Chandra* and XMM-Newton.

The X-ray emission of 3C 346 and its environment

D.M. Worrall¹ and M. Birkinshaw¹

Department of Physics, University of Bristol, U.K.

`d.worrall@bristol.ac.uk`

ABSTRACT

We present a detailed analysis of the X-ray properties of 3C 346, combining information from ROSAT and ASCA. The dominant component of X-ray emission ($\sim 10^{44}$ ergs s⁻¹ in each of the 0.5-3 keV and 2-10 keV bands) is unresolved and not heavily absorbed (intrinsic $N_{\text{H}} \lesssim 2 \times 10^{21}$ cm⁻²), with evidence for variability of $32 \pm 13\%$ over 18 months. We relate the X-ray emission to radio structures on both milliarcsecond scales and the arcsecond scales which *Chandra* can resolve. The absence of X-ray absorption, and the radio/optical/X-ray colors, when combined with previous radio evidence that the source is a foreshortened FR II, suggest that the radio jets are seen at an angle to the line of sight of about 30° , intermediate between the radio-galaxy and quasar classes. We place an upper limit of 5.6×10^{43} ergs s⁻¹ on the 2-10 keV luminosity of any central X-ray component absorbed by gas which might be obscuring the broad-line emission region. Roughly a third of the soft X-ray emission is from a cluster atmosphere, for which we measure a temperature of $1.9_{-0.7}^{+1.3}$ keV, making this the only low-redshift ($z < 0.2$) powerful radio galaxy other than Cygnus A with a measured cluster temperature. At a jet angle of $\sim 30^\circ$, all the radio structures lie within the core radius of the cluster, for which the cooling time is sufficiently long that there is no reason to expect the presence of a cooling flow. The radio lobes of 3C 346 are roughly in pressure balance with the external medium under the assumptions that the energy densities in the magnetic field and radiating particles balance and that a source of excess pressure in the radio lobes, commonly invoked in other radio galaxies, is absent here.

Subject headings:

1. Introduction

3C 346 is a well-known compact radio source in a 17th magnitude galaxy at $z = 0.161$ (e.g. Laing et al. 1983). Although originally classified as a member of the physically small class of

¹Harvard-Smithsonian Center for Astrophysics, Cambridge, MA 02138

Compact Steep Spectrum (CSS) radio sources (Fanti et al. 1985), Spencer et al. (1991) argue that its luminous core and small, one-sided (eastwards), distorted jet structure are best explained by the foreshortening of a normal radio galaxy by a combination of relativistic beaming and small angle to the line of sight. The radio morphology then suggests it would be a member of the FRII class, as defined by Fanaroff & Riley (1974), and this is consistent with its 178 MHz power of $10^{26} \text{ W Hz}^{-1} \text{ sr}^{-1}$, about a factor of five higher than the fuzzy boundary between sources exhibiting FRI structure and those classed as FRIIs. Subsequent authors have generally supported the foreshortened FRII picture, and in particular Cotton et al. (1995) use the VLBI radio-core dominance and jet-to-counterjet ratio to infer an angle to the line of sight of $\theta < 32^\circ$, and a speed relative to that of light of $\beta > 0.8$. Unified Models (e.g. Barthel 1989) class FRII radio sources with their jets this close to the line of sight as quasars in contrast to radio galaxies, and so the absence of an expected strong broad emission-line region (BELR) needs explanation. Dey & van Breugel (1994) combine their upper limit for the flux of $H\beta$ with the emission-line flux of $H\alpha + [\text{N II}]$ from narrow-band imaging data of Baum et al. (1988) to suggest that the nuclear regions are seen through a large extinction ($A_v > 8 \text{ mag}$), such that the BELR may only be detectable in the infrared. However, such a large extinction would then be unusual for a source of 3C 346’s presumed orientation.

At high radio frequencies (15 GHz), 3C 346’s one sided wiggly jet breaks into a series of bright knots which van Breugel et al. (1992) label as B, C, D, and E with increasing distance from the core. The brightest knot, C, at $\sim 3''$ east of the radio core may reside outside the optical galaxy if the jet is indeed at a small angle to the line of site. Dey & van Breugel (1994) detected excess emission in ground-based U and red images which they attributed to knot C and its nearby companion, knot B. More recently an HST snapshot image with the WFPC2 has provided a spectacular view of the jet at optical wavelengths (F702W filter: $\sim 6000 - 8000 \text{ \AA}$), with a one-to-one correspondence between optical and radio features in the jet, including knots B, C, and D (de Koff et al. 1996; de Vries et al. 1997).

3C 346 was detected in the X-ray with the *Einstein* IPC, yielding 136 ± 13 counts in 2.9 ks, and giving a 0.5-3 keV luminosity of $1.4 \times 10^{44} \text{ ergs s}^{-1}$ to within an estimated $\sim 30\%$ uncertainty (Fabbiano et al. 1984). Subsequent longer observations were made with the ROSAT PSPC, which permitted Hardcastle & Worrall (1999) to show that the X-ray emission is a composite of resolved and unresolved components, and with ASCA, from which Sambruna et al. (1999) derived a power-law spectral index for the overall X-ray emission as part of a statistical study of the X-ray emission from a number of radio-loud active galaxies. In this paper we present a detailed analysis of the X-ray properties, combining information from ROSAT and ASCA (§2). We discuss the pressure and cooling time of the cluster gas which gives rise to the extended X-ray emission (§3), and we discuss the likely origin of the unresolved X-ray emission in the context of what is known from radio and optical measurements (§4). Our conclusions are in §5.

Throughout the paper we adopt a Friedmann cosmological model with $H_0 = 50 \text{ km s}^{-1} \text{ Mpc}^{-1}$, $q_0 = 0$. At the redshift of 3C 346, 10 arcsec corresponds to 37.5 kpc.

2. X-ray Analysis and Results

Dates and exposure times for the ROSAT and ASCA X-ray observations are given in Table 1. Our analysis made use of the IRAF/Post Reduction Off-line Software (PROS) for ROSAT and FTOOLS and XSPEC for ASCA. The ASCA data are from the two Gas Imaging Spectrometers (GIS) and the two Solid-State Spectrometers (SIS). The SIS data were taken in a mixture of 2-CCD faint and bright mode; the faint-mode data were converted to bright mode by the standard processing software before analysis. Our screening used standard recommended procedures, and values adopted included an elevation angle > 5 degrees for dark earth (and 12 degrees for bright earth with the SIS), and a cut-off rigidity of 6 GeV/c for the SIS and 4 GeV/c, with extra screening, for the GIS. Four 8-sec intervals of anomalously high background counts in the SIS1 were excluded from the data. Our spatial analysis of the ROSAT data used generalized software (Birkinshaw 1994; Worrall & Birkinshaw 1994) for fitting radial profiles to combinations of models convolved with the instrument Point Response Function (PRF).

2.1. ROSAT Spatial and Spectral Results

The ROSAT PSPC image centered on 3C 346 is shown as a contour plot in in Figure 1. A re-registration of the X-ray image by 5 arcsec (within ROSAT’s absolute positional accuracy) aligns the centroid of the X-ray emission with the radio core of 3C 346, and the X-ray source 3.34 arcmin to 3C 346’s northeast with a star of late-type color index listed in the USNO catalog ($R=12.8$ mag, $B=15.2$ mag). The northeast source, at an X-ray flux of $\sim 6 \times 10^{-14}$ ergs cm $^{-2}$ s $^{-1}$ (0.2 - 2 keV), has an X-ray-to-optical flux ratio consistent with the range measured for late-type stars in the EMSS survey (e.g. Sciortino et al. 1995), and, although there are insufficient counts to constrain well the X-ray spectrum, it can be fitted with gas components of temperature $\sim 2 \times 10^6$ and $\sim 10^7$ K, consistent with findings for late-type stellar coronae (Preibisch 1997).

Figure 2 shows the X-ray radial profile that we extracted for 3C 346, excluding a circle of radius $2'$ around the source to the northeast. The boundaries of the 23 bins were selected so as to give at least 20 counts per bin, and only counts in the energy band 0.2-1.9 keV, where the PRF is well modelled, were used. Background was measured from an annulus of radii 3 and 5.7 arcmin, again excluding the nearby source. A fit of this radial profile to the PRF gives an unacceptable χ^2 of 208, indicating the presence of extended X-ray emission, whereas the X-ray source to the northeast is consistent with being point-like. A single-component β -model², a description of gas in hydrostatic equilibrium (e.g. Sarazin 1986), also gives a poor fit to the emission centered on 3C 346, with $\chi^2_{\min} \sim 40$ for $\beta \sim 0.5$ and an unacceptably small core radius of < 0.05 arcsec. The composite of a point source and β -model gives acceptable fits which are relatively insensitive to the value of β , which is itself highly correlated with core radius, θ_{cx} (Fig. 2). In Hardcastle & Worrall (1999)

²Counts per unit area per unit time at radius θ proportional to $(1 + \frac{\theta^2}{\theta_{\text{cx}}^2})^{0.5-3\beta}$.

we present results for one set of acceptable parameters. Here we extend that work by exploring the uncertainties in physical parameters resulting from the full range in spatial and spectral model parameters.

Figure 3 shows χ^2 as a function of counts in the unresolved component and in the β model (out to a radius of $3'$), where each cross shows the minimum value of χ^2 for a given trial combination of β and θ_{cx} , where the model normalizations are free parameters of the fit. Fits are performed over a broader range of β and θ_{cx} than shown in the left-hand plot of Figure 3, such that all combinations of parameters giving a particular value of χ^2 (less than $\chi_{\text{min}}^2 + 5$) are adequately sampled. The model being fitted to the data has four parameters (point-source normalization, beta-model normalization, β , and θ_{cx}), and in principle could be written in such a way as to make any quantity which is dependent on one or more of these four parameters to be itself a parameter of the model. In practice, the trade-off between computing time and programming time makes it more efficient to use the brute-force method of computing χ^2 for many parameter-value combinations and plotting χ^2 as a function of the quantity of interest, as shown in Figures 3 and 4.

The counts in the point-source model are highly correlated with the counts in the β model and so, since we are interested in comparing the division of counts between the two components found in this spatial analysis with spectroscopic results, our 1σ errors are given by $\chi_{\text{min}}^2 + 2.3$ (1σ for two interesting parameters). Our spatial fitting thus finds 736_{-34}^{+21} ROSAT PSPC counts (0.2-1.9 keV) in the unresolved component, and 371_{-46}^{+104} in resolved emission out to a radius of $3'$ (including the $\sim 18\%$ correction for missing counts from the region of the nearby source to the northeast). The resolved emission is well concentrated within a radius of $3'$, as indicated by the shape of the radial profile and the preference for values of β close to unity (Fig. 2); extending the radius to $4'$ increases the counts in the β model only by 5.6%.

Spectral fits to the ROSAT PSPC data (over the same spatial on-source and background regions as used in our spatial analysis, but over a broader energy range) give acceptable fits to either a power law of energy index 0.75 ($\chi_{\text{min}}^2 = 18.2$ for 23 degrees of freedom) or a Raymond-Smith thermal model with 30% solar abundances and $kT = 2.9$ keV ($\chi_{\text{min}}^2 = 18.3$). In neither case is excess absorption over the column density through the Galaxy required, with 3σ upper limits of $1.7 \times 10^{21} \text{ cm}^{-2}$ and $6 \times 10^{20} \text{ cm}^{-2}$ for the power-law and thermal models, respectively. Interestingly, while a combination of power-law and thermal spectral components does not decrease χ^2 sufficiently to argue, using an F-test, that two components are required based on the spectral analysis alone, the two-component fit settles on parameters which give roughly the same division of counts between the power-law and thermal components as did the spatial analysis between the unresolved and resolved components, respectively.

Since the extracted spectrum should contain all the counts from the unresolved component, we performed two-component spectral fits with the single additional requirement that the power-law component provide between 702 and 757 counts between 0.2 and 1.9 keV. For these fits, the hydrogen column density was fixed at the Galactic value (since single-component fits required no

excess absorption), and abundances were fixed at 30%, the typical value for cluster gas (Arnaud et al. 1992). The fits constrained the temperature of the gas to be $kT = 1.9^{+1.3}_{-0.7}$ keV and the power-law energy index, α , ($f_\nu \propto \nu^{-\alpha}$) to be $0.69^{+0.16}_{-0.14}$ (other temperature and slope combinations being inconsistent with the required counts in the power-law model). Tables 2 and 3 summarize the results for the cluster gas and unresolved (power-law) emission (which we attribute to the active galaxy). The tables include the luminosities in various spectral bands, where the uncertainties are dominated by the errors in counts represented in Figure 3.

Now that we have measured a gas temperature, we return to the spatial fits to compute other parameters of interest (Table 2) such as the central pressure and density, and their equivalents at a radius of $10''$, roughly the projected outer radius of the radio lobes, which appear as an elliptical halo around the resolved jet features (van Breugel et al. 1992). Figure 4 is a similar plot to Figure 3, but for central gas pressure, assuming a temperature of $kT = 1.9$ keV. For kT between 1.2 and 3.2 keV, the PSPC count-rate per unit emission measure is independent of temperature, to within the statistical uncertainties. This means that our density measurements are unaffected by the temperature uncertainty, whereas the pressure and cooling-time errors given in Table 2 have been increased to include a contribution from the temperature range, since pressure is $\propto kT$ and cooling time is approximately $\propto \sqrt{kT}$.

2.2. ASCA Spectral Results using ROSAT Spatial Analysis

ROSAT has found that the soft X-ray emission from 3C 346 divides roughly as two-thirds point-like and one-third extended emission concentrated within a radius of $\sim 3'$. Visual inspection of the ASCA images showed no evidence for resolved X-ray emission, consistent with ASCA's larger PRF as compared with ROSAT. For the results presented here, we extracted spectra from circular regions centered on the source position, using a radius of $4'$ for the SIS, and the larger value of $6'$ for the GIS to accommodate this detector's contribution to the PRF. Background was measured from off-source regions on the images. Although the location of the X-ray emitting star to the northeast of 3C 346 (Fig. 1) falls within our on-source regions, the X-ray emission is weak and soft compared with that from 3C 346, and contamination in ASCA's somewhat harder spectral band is estimated to be negligible. Spectra were rebinned to a minimum of 20 counts per bin before we performed χ^2 fitting of the SIS and GIS data jointly to various models. We followed the recommended procedure of excluding energies below 0.6 keV (0.4 keV for the SIS) and above 10 keV, where the detector spectral responses are uncertain.

As is the case for ROSAT, the data give an acceptable fit to a single-component power law with no excess absorption over the line-of-sight column density through our galaxy ($\chi^2 = 159$ for 154 degrees of freedom). Uncertainty contours for power-law photon index ($\alpha + 1$) and normalization are shown in Figure 5. Our spectral-index measurement of 1.95 ± 0.11 ($\chi^2_{\min} + 2.7$), upon which the GIS and SIS separately agree well, is a little steeper than that found independently by Sambruna et al. (1999) from the same observation (1.81 ± 0.12), but results agree within the uncertainties.

Excess intrinsic absorption is less well constrained than with ROSAT, and the 3σ upper limit on line of sight hydrogen column density is $2.9 \times 10^{21} \text{ cm}^{-2}$.

Although we know from the spatial analysis of the ROSAT data that a single component power law is an inadequate description of the X-ray emission from 3C 346, it is instructive to compare the ROSAT and ASCA results for this spectral model. Figure 5 provides the first indication that the X-ray emission may have varied between the ROSAT and ASCA observations.

The statistical errors on the ASCA data are too large to constrain well the parameters for a two-component, power law and thermal, fit. We have therefore fixed the thermal component to be within the temperature and normalization bounds determined using the ROSAT data. Figure 6 compares the ASCA-derived uncertainties in power-law normalization and photon spectral index with the range found from ROSAT. This provides evidence for the power-law component having decreased by $\sim 32 \pm 13\%$ between the ROSAT and ASCA measurements.

The only other X-ray measurement of which we are aware is that with the *Einstein* Observatory reported by Fabbiano et al. (1984). Our estimates of the total 0.5-3 keV luminosity from ROSAT and ASCA (Tables 2 and 3) of $1.4_{-0.2}^{+0.4} \times 10^{44} \text{ ergs s}^{-1}$ and $1.1_{-0.3}^{+0.4} \times 10^{44} \text{ ergs s}^{-1}$, respectively, are both consistent with the *Einstein* luminosity of $1.4 \pm 0.4 \times 10^{44} \text{ ergs s}^{-1}$.

3. The Cluster Gas

Table 2 summarizes the properties of the X-ray emitting gas. 3C 346 is the only low-redshift ($z < 0.2$) powerful radio galaxy other than Cygnus A (3C 405) with a measured cluster temperature. Indeed, the X-ray atmospheres around most powerful radio galaxies at low redshift are currently undetected, although for ROSAT-observed sources there is some evidence that gas may well be present at levels close to the X-ray upper limits (Hardcastle & Worrall 2000b). The cluster around Cygnus A is considerably hotter and richer than that around 3C 346, whose atmosphere is more similar to that around a typical low-power (FRI) radio galaxy (Fig. 7). The cooling time of 3C 346's cluster atmosphere (Table 2) is sufficiently long that there is no reason to invoke the presence of a cooling flow. Optical evidence for cluster membership is presented by Zirbel (1997), who classifies the cluster as Bautz-Morgan class I, with a richness of 10 ± 4.6 .

The southwest radio lobe, modelled as lying at an angular distance between $0''$ and $10''$ from the core, is estimated to have a minimum pressure in magnetic field and radiating particles of $10^{-11} \text{ dynes cm}^{-2}$ (Hardcastle & Worrall 2000b). The closeness of this value to the gas pressure (Table 2) may suggest a finely tuned pressure-confined source. However, in other X-ray detected FRIs (Hardcastle & Worrall 2000b) and most FRI radio galaxies (e.g. Worrall & Birkinshaw 2000) the thermal pressure of the atmosphere exceeds the minimum-energy radio pressure and, since this would stifle the radio source, an additional dominant component of internal pressure is usually invoked, such as assuming the source is out of equipartition or that there is a pressure contribution from non-radiating particles. If this were the case for 3C 346, the radio structures

would be overpressured, and we would expect lateral expansion of the lobes. An angle to the line of sight between about 10 and 20 degrees would mitigate the effect slightly (increasing the ratio of thermal to radio pressure by about 50%), since the minimum radio pressure (calculated assuming the radio structures are in the plane of the sky) would decrease while the thermal pressure would be barely affected, with the source still lying within the core radius of the cluster. Until more detailed measurements are available, 3C 346 remains a candidate for a source which, under minimum-energy assumptions, is just in pressure balance with the external medium.

4. The Unresolved X-ray Emission

Unresolved emission dominates the X-radiation at both ROSAT and ASCA energies. The measurements are summarized in Table 3. The fact that the unresolved emission is not heavily absorbed (with an upper limit of $\sim 2 \times 10^{21} \text{ cm}^{-2}$) means either that it is nonthermal and related to the radio structures on VLBI to arcsec scales, or that the central AGN regions are not hidden by obscuration. In either case, X-ray variability of about 30% over 18 months would favor an angle to the line of sight of $\lesssim 30^\circ$, reinforcing previous claims that this source is a foreshortened FR II, and suggesting it should be considered more closely related to the quasar than radio-galaxy class.

The absence of broad $H\beta$ is then unusual. Explaining this by an extinction of $A_v = 8 \text{ mag}$ (Dey & van Breugel 1994), and adopting the gas to dust ratio applicable to our own galaxy, implies that the broad-line regions, and so too presumably the AGN, lie beyond gas which provides a line of sight Hydrogen column density of $N_H = 1.4 \times 10^{22} \text{ cm}^{-2}$ (Burstein & Heiles 1978). We have placed an upper limit on an X-ray component this heavily obscured by fitting the ASCA data to thermal emission (fixed as before) together with two power-law components, one of which is absorbed by $N_H = 1.4 \times 10^{22} \text{ cm}^{-2}$ and one of which suffers no intrinsic absorption in the source. These fits were run for two adopted spectral indices for the absorbed power law: $\alpha = 0.7$ and $\alpha = 1$ (photon index of 1.7 and 2.0). In neither case were the fitted spectral indices and normalizations for the unabsorbed emission much changed from Figure 6, although the uncertainties in spectral index increased as expected, particularly to allow steeper slopes. Although on the basis of an F-test there is no justification for including the extra (absorbed) component, the 90% upper limits on its intensity are quite high: in units of photons $\text{cm}^{-2} \text{ s}^{-1} \text{ keV}^{-1}$ at 1 keV, the normalizations are 1.25×10^{-4} and 1.9×10^{-4} for slopes of $\alpha = 0.7$ and 1.0, respectively. These values correspond to an upper limit on the pre-absorption 2-10 keV X-ray luminosity of $5.6 \times 10^{43} \text{ ergs s}^{-1}$, or about 50% as luminous as the detected X-rays. More sensitive high-energy X-ray measurements are required to investigate whether such an absorbed central X-ray component is present in 3C 346.

It seems reasonable that the unabsorbed unresolved X-ray emission comes primarily from the inner regions of the radio jet, within an arcsec of the core (Worrall 1997). Indeed, the ratio of 3C 346's radio-core and unresolved-X-ray flux densities are in agreement with those for other 3CRR radio galaxies and quasars, from which we have made a statistical argument that each source has a beamed nuclear soft X-ray component directly related to the radio core (Hardcastle &

Worrall 1999). In common with other 3CRR radio galaxies and quasars, the core radio spectrum is flat, with VLA flux densities of 220 mJy at 5 GHz and 243 mJy at 15 GHz, and a 5 GHz VLBI measurement of 165 mJy (van Breugel et al. 1992; Giovannini et al. 1990). An optical core component of 37.5 μ Jy at 7000 Å has been separated from the galaxy in HST data by Chiaberge et al. (1999). Combined with our X-ray measurements, these results imply interpolated two-point spectral indices of $\alpha_{\text{ro}} = 0.76$, $\alpha_{\text{ox}} = 0.86$, and $\alpha_{\text{rx}} = 0.8$. These values place 3C 346 within the color range of low-power FRI radio galaxies (Hardcastle & Worrall 2000a), whereas radio-loud quasars from 3CRR typically have steeper values of α_{ox} , in the range 1.0 to 1.6 (Wilkes et al. 1994). The spectral energy distribution therefore argues that the viewing angle to 3C 346 is probably not too much smaller than 30° , placing it on the boundary between a radio galaxy and quasar.

It is likely that a significant fraction of the X-ray emission which is unresolved to ROSAT and ASCA actually comes from the radio and optical knots, and in particular the brightest of these, knot C, $3''$ from the core. The radio spectral index in the knot between 1.6 and 15 GHz (Spencer et al. 1991; Dey & van Breugel 1994; van Breugel et al. 1992) is roughly $\alpha = 0.5$, consistent with synchrotron emission from an electron population which is energized by first-order Fermi acceleration at strong shocks. The optical flux-density (de Vries et al. 1997) is below an $\alpha = 0.5$ extrapolation from 15 GHz, implying an energy-loss break in the electron spectrum. Modelling the knot as a sphere of radius 165 pc, based on the 15 GHz measurements (van Breugel et al. 1992), we find a good fit to the radio and optical data for an equipartition magnetic field of $\sim 650 \mu\text{Gauss}$ and an electron spectral index which breaks by unity at 10^{10} eV. If, as is likely, the electron spectrum extends to 10^{13} eV, we expect significant X-ray synchrotron emission from the knot, amounting to roughly 10% of the total unresolved emission. This should be easily detectable with *Chandra*, which has the spatial resolution to separate the core and jet. *Chandra* observations will also make a strong test of the equipartition assumption, something which results for the quasar jet in PKS 0637-752 have now dramatically brought into question (Chartas et al. 2000; Schwartz et al. 2000). If the X-ray emission in 3C 346's knot is above the synchrotron predictions then we will be forced to infer a Compton-scattering origin, and most likely a synchrotron self-Compton origin, at levels too high for equipartition predictions but in line with results for PKS 0637-752. In this case an even higher fraction of the unresolved X-rays might originate in the jet.

5. Conclusions

ROSAT and ASCA measurements of the nearby powerful radio source 3C 346 find extended emission, consistent with a cluster atmosphere, and unabsorbed unresolved emission, consistent with non-thermal radiation from radio structures on VLBI to arcsecond scale sizes. We measure a temperature of $1.9_{-0.7}^{+1.3}$ keV for the extended emission, making this the only low-redshift ($z < 0.2$) powerful radio galaxy other than Cygnus A with a measured cluster temperature. The temperature and luminosity of the cluster gas are consistent with the correlation found for the atmospheres around nearby, less powerful, radio galaxies (Fig. 7). The cooling time for the cluster gas is too

long for a significant cooling flow to have become established. The radio lobes of 3C 346 are roughly in pressure balance with the external medium under the assumptions that the energy densities in the magnetic field and radiating particles balance, and that a source of excess pressure in the radio lobes, commonly invoked in other radio galaxies, is absent here.

3C 346's orientation to the line of sight is uncertain. It was originally classified as being an intrinsically small member of the CSS class, but radio measurements have since been used to infer a jet-angle to the line of sight of $\theta < 32^\circ$. The evidence that the unresolved X-ray flux is not only unabsorbed but has varied by $32 \pm 13\%$ over 18 months makes it likely that a significant fraction of this emission is from deep in the radio jets, in sub-arcsec regions and influenced by relativistic beaming, which would support a small angle to the line of sight. However, the radio/optical/X-ray colors are not those of a quasar, rather they are similar to those of other nearby radio galaxies, and so we support the idea that this source is at an orientation intermediate between quasars and radio galaxies.

3C 346 is one of a relatively small number of radio galaxies where optical emission has been detected from the radio jet. We predict that the brightest knot in the jet is detectable with *Chandra*, and observations will test the equipartition assumptions which have been challenged recently by the *Chandra* observations of PKS 0637-752. *Chandra* observations are also required to probe the possible presence of an additional heavily absorbed X-ray emission component of $< 5.6 \times 10^{43}$ ergs s^{-1} (2-10 keV), where the absorption is due to the gas suggested to be obscuring the broad-line emission regions in this source.

We acknowledge support from NASA grant NAG 5-2961.

REFERENCES

- Arnaud, M. & Evrard, A.E. 1999, MNRAS, 305, 631
- Arnaud, M., Rothenflug, R., Boulade, O., Vigroux, L. & Vangioni-Flam, E. 1992, A&A, 254, 49
- Barthel, P.D. 1989, ApJ, 336, 606
- Baum, S.A., Heckman, T.M. & van Breugel, W.J.M. 1988, ApJS, 68, 643
- Birkinshaw, M. 1994, in *Astronomical Data Analysis Software and Systems III*, ASP Conference Series Volume 61, eds. D.R. Crabtree, R.J. Hanisch & J. Barnes, 249.
- Burstein, D. & Heiles, C. 1978, ApJ, 225, 40
- Chartas, G. et al. 2000, ApJ, in press.
- Chiaberge, M., Capetti, A. & Celotti, A. 1999, A&A, 349, 77
- Cotton, W.D., Feretti, L., Giovannini, G., Venturi, T., Lara, L., Marcaide, J. & Wehrle, A.E. 1995, ApJ, 452, 605
- de Koff, S., Baum, S.A., Sparks, W.B., Biretta, J., Golombek, D., Macchetto, F., McCarthy, P. & Miley, G.K. 1996, ApJS, 107, 621
- de Vries, W.H., O'Dea, C.P., Baum, S.A., Sparks, W.B., Biretta, J., de Koff, S., Golombek, D., Lehnert, M.D., Macchetto, F., McCarthy, P. & Miley, G.K. 1997, ApJS, 110, 191
- Dey, A. & van Breugel, W.J.M. 1994, AJ, 107, 1977
- Fabbiano, G., Miller, L., Trinchieri, G., Longair, M. & Elvis, M. 1984, ApJ, 277, 115
- Fanaroff, B.L. & Riley, J.M. 1974, MNRAS, 167, 31P
- Fanti, C., Fanti, R., Parma, P., Schilizzi, R.T. & van Breugel, W.J.M. 1985, A&A, 143, 292
- Giovannini, G., Feretti, L. & Comoretto, G. 1990, ApJ, 358, 159
- Hardcastle, M.J. & Worrall, D.M. 1999, MNRAS, 309, 969
- Hardcastle, M.J. & Worrall, D.M. 2000a, MNRAS, 314, 359
- Hardcastle, M.J. & Worrall, D.M. 2000b, MNRAS, submitted
- Helsdon, S.F. & Ponman, T.J. 2000, MNRAS, 315, 356
- Laing, R.A., Riley, J.M. & Longair, M.S. 1983, MNRAS, 204, 151
- Preibisch, T. 1997, A&A, 320, 525

- Sambruna, R.M., Eracleous, M. & Mushotzky, R.F. 1999, ApJ, 526, 60
- Sarazin, C.L. 1986, Rev. Mod. Phys., 58, 1
- Sciortino, S., Favata, F. & Micela, G. 1995, A&A, 296, 370
- Schwartz, D.A. et al. 2000, ApJ, letters, submitted.
- Spencer, R.E., Schilizzi, R.T., Fanti, C., Fanti, R., Parma, P., van Breugel, W.J.M., Venturi, T., Muxlow, T.W.B. & Rendong, N. 1991, MNRAS, 250, 225
- Stark, A.A., Gammie, C.F., Wilson, R.W., Bally, J., Linke, R.A., Heiles, C. & Hurwitz, M. 1992, ApJS, 79, 77
- van Breugel, W.J.M., Fanti, C., Fanti, R., Stanghellini, C., Schilizzi, R.T. & Spencer, R.E. 1992, A&A, 256, 56
- Wilkes, B.J., Tananbaum, H., Worrall, D.M., Avni, Y., Oey, M.S. & Flanagan, J. 1994, ApJS, 92, 53
- Worrall D.M. 1997, in *Relativistic Jets in AGNs*, ed. M. Ostrowski, M. Sikora, G. Madjeski & M. Begelman (Astronomical Observatory of the Jagiellonian University, Krakow), 20 (astro-ph/9709165)
- Worrall, D.M. & Birkinshaw, M. 1994, ApJ, 427, 134
- Worrall, D.M. & Birkinshaw, M. 2000, ApJ, 530, 719
- Zirbel, E.L. 1997, ApJ, 476, 489

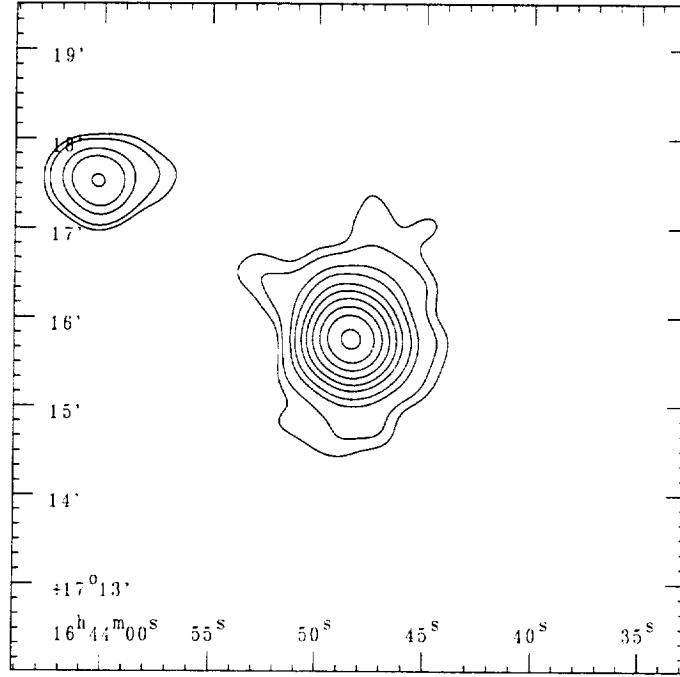


Fig. 1.— ROSAT PSPC image centered on 3C 346, in J2000 equatorial coordinates. Data have been smoothed with a Gaussian of $\sigma = 12$ arcsec. Pixels are 0.5×0.5 arcsec square, and the lowest contour corresponds to 3σ significance. Contour levels, in cts/pixel, are 0.003, 0.004, 0.007, 0.01, 0.016, 0.023, 0.034, 0.05, 0.07 and 0.1. 3C 346's radio and optical jet structures span an angular size less than 4 arcsec (see text), and lie well within the PRF of the ROSAT PSPC, as does the combined optical extent of 3C 346's host galaxy and its nearby companion (de Koff et al. 1996). Lower-frequency (1.5 GHz) radio emission extends over a region $\sim 14'' \times 12''$ (van Breugel et al. 1992), also within the X-ray PRF.

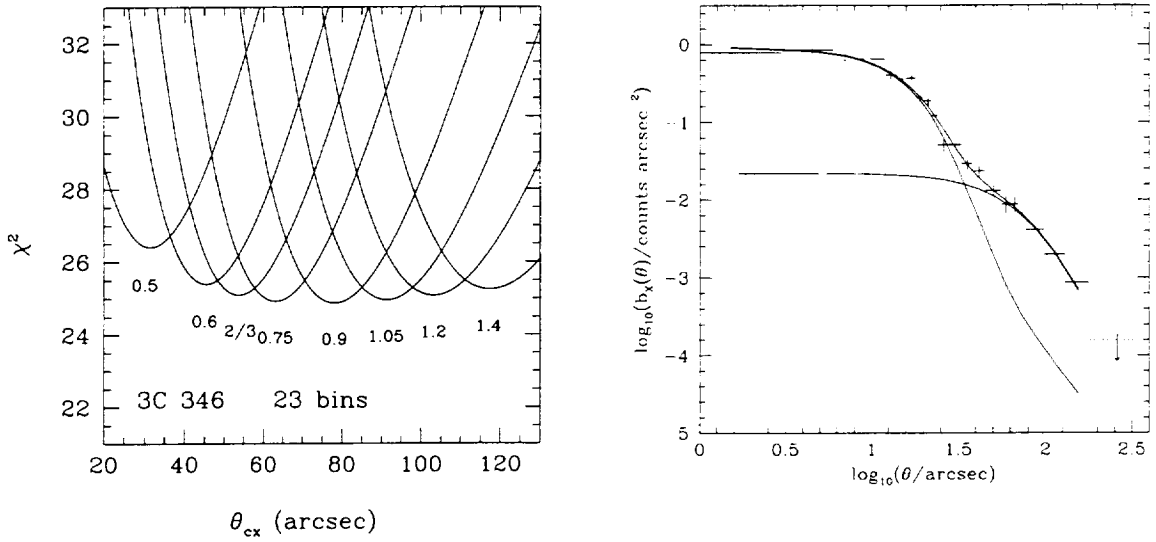


Fig. 2.— Result of fitting a β -model plus point source to the PSPC radial profile of 3C 346. Left: - χ^2 versus core radius of the β model, for different values of β . The fits are relatively insensitive to the value of β which is highly correlated with core radius, θ_{cx} . Right: - data show the background-subtracted radial profile, and solid curves the two model components of the best-fit model. The β -model is for $\beta = 0.9$, $\theta_{cx} = 78''$. The dotted line shows the contribution of the model to the background region, as taken into account in the fitting.

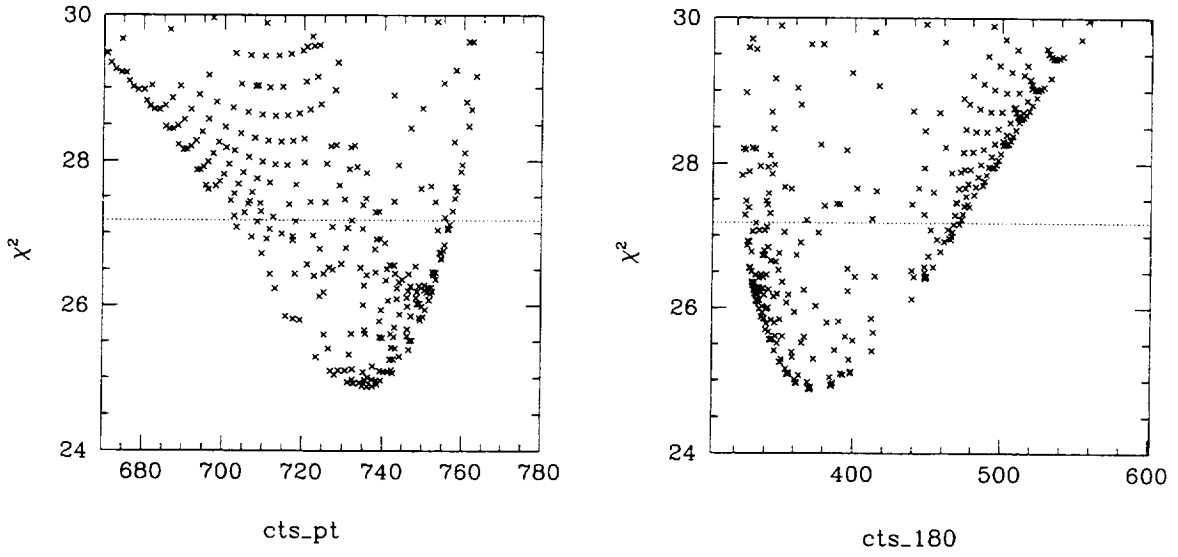


Fig. 3.— ROSAT PSPC counts in the unresolved component, *cts_pt* (Left) and the β model (out to a radius of $3'$ and including the $\sim 18\%$ correction for missing counts from the region of the nearby source to the northeast, *cts_180*: Right) from the two-component spatial analysis. In each plot, a cross marks the position for a fit of chosen β and θ_{cx} (where the normalizations of the two model components were free parameters of the fit), and necessarily large ranges of β and θ_{cx} were sampled to provide full ranges in *cts_pt* and *cts_180* for all values of χ^2 shown. The dotted lines are at $\chi^2_{\text{min}} + 2.3$, corresponding to 1σ for two interesting parameters.

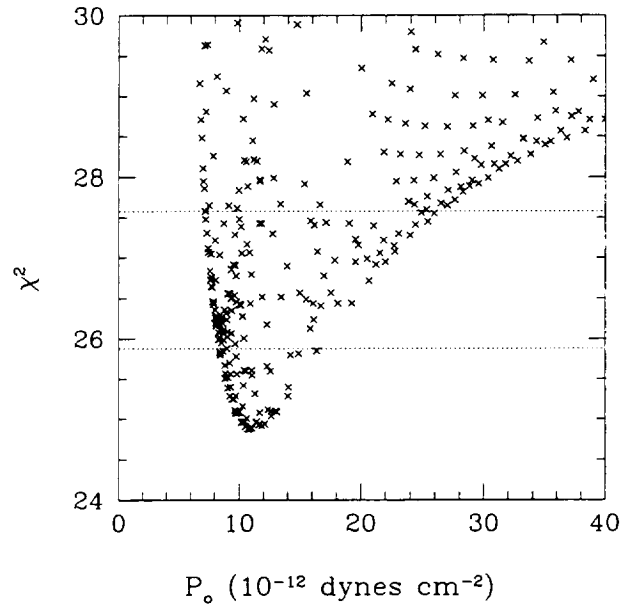


Fig. 4.— Similar to Figure 3 but for central gas pressure. Dotted lines are at $\chi_{\min}^2 + 1$ and $\chi_{\min}^2 + 2.7$, corresponding to 1σ and 90% confidence, respectively, for one interesting parameter. An additional error in central gas pressure contributes to the value in Table 2 due to the uncertainty in temperature.

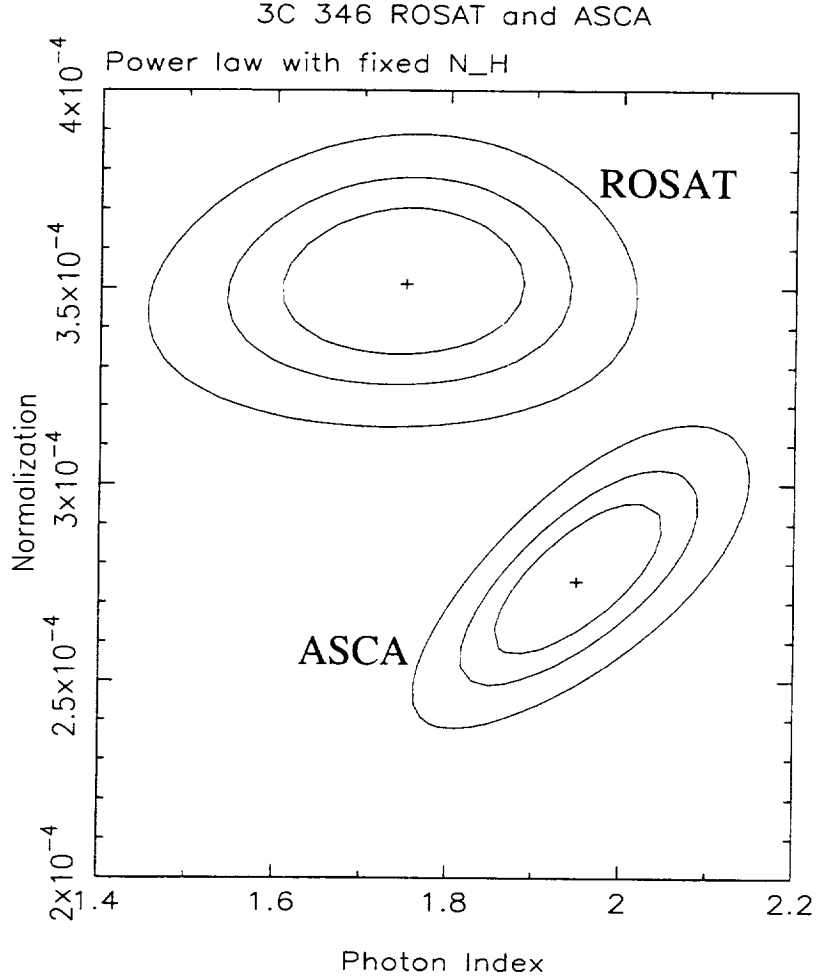


Fig. 5.— Uncertainties in normalization and power-law photon index ($\alpha + 1$) for single-component power-law spectral fits to the ROSAT PSPC (upper contours) and ASCA combined SIS and GIS data (lower contours). The contours are at $\chi^2_{\min} + 2.3$, 4.61 and 9.21, corresponding to confidence levels of 1σ , 90% and 99% for two interesting parameters. The contours do not overlap, suggesting a combination of source variability and the model being inadequate to describe the data, which are known from the spatial analysis to include thermal emission.

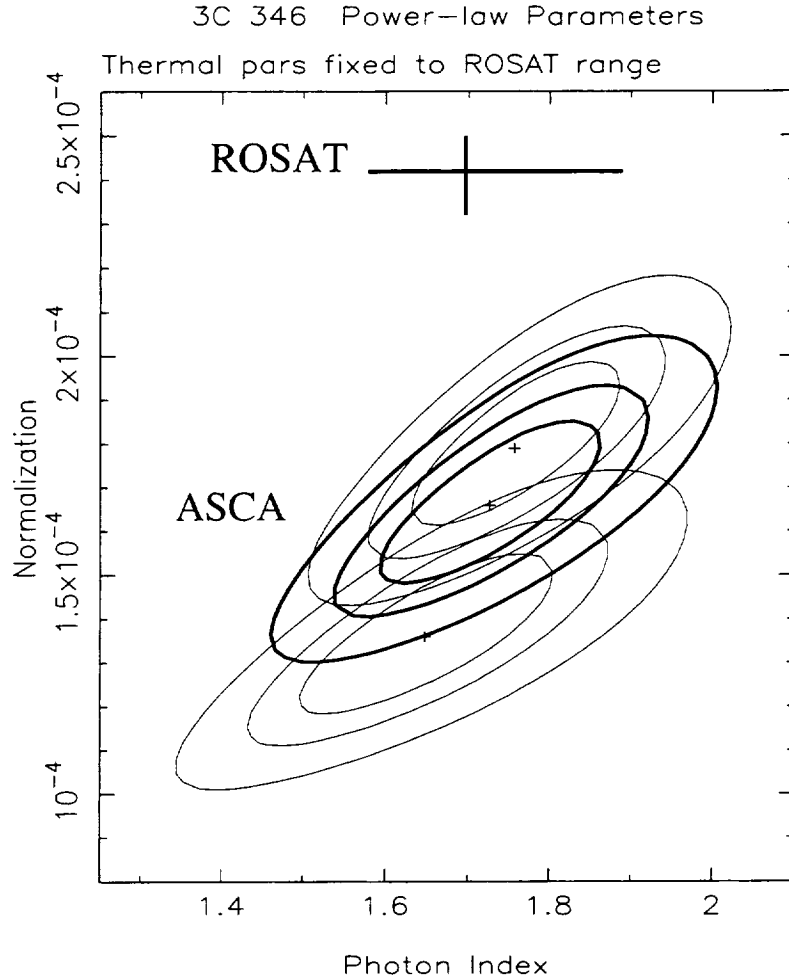


Fig. 6.— Uncertainties in power-law normalization and photon index ($\alpha + 1$) for two-component (thermal plus power-law) spectral fits to the ASCA combined SIS and GIS data. The contours are at $\chi^2_{\min} + 2.3, 4.61$ and 9.21 , corresponding to confidence levels of 1σ , 90% and 99% for two interesting parameters. The set of heavy contours are where the thermal spectrum is fixed to the best-fit parameters from the ROSAT analysis. The two other sets of contours correspond to the upper and lower bounds on the thermal component as deduced from ROSAT, taking into account both statistical and modelling uncertainties. The normalization is in units of photons $\text{cm}^{-2} \text{s}^{-1} \text{keV}^{-1}$ at 1 keV: a normalization of 10^{-4} corresponds to $0.0663 \mu\text{Jy}$. The ROSAT analysis finds a photon index of $1.69^{+0.16}_{-0.14}$ and a normalization between 2.33×10^{-4} and 2.5×10^{-4} (1σ for two interesting parameters). This suggests that the power-law component decreased in intensity by $\sim 30\%$ between the ROSAT and ASCA observations, while staying roughly constant in spectral slope.

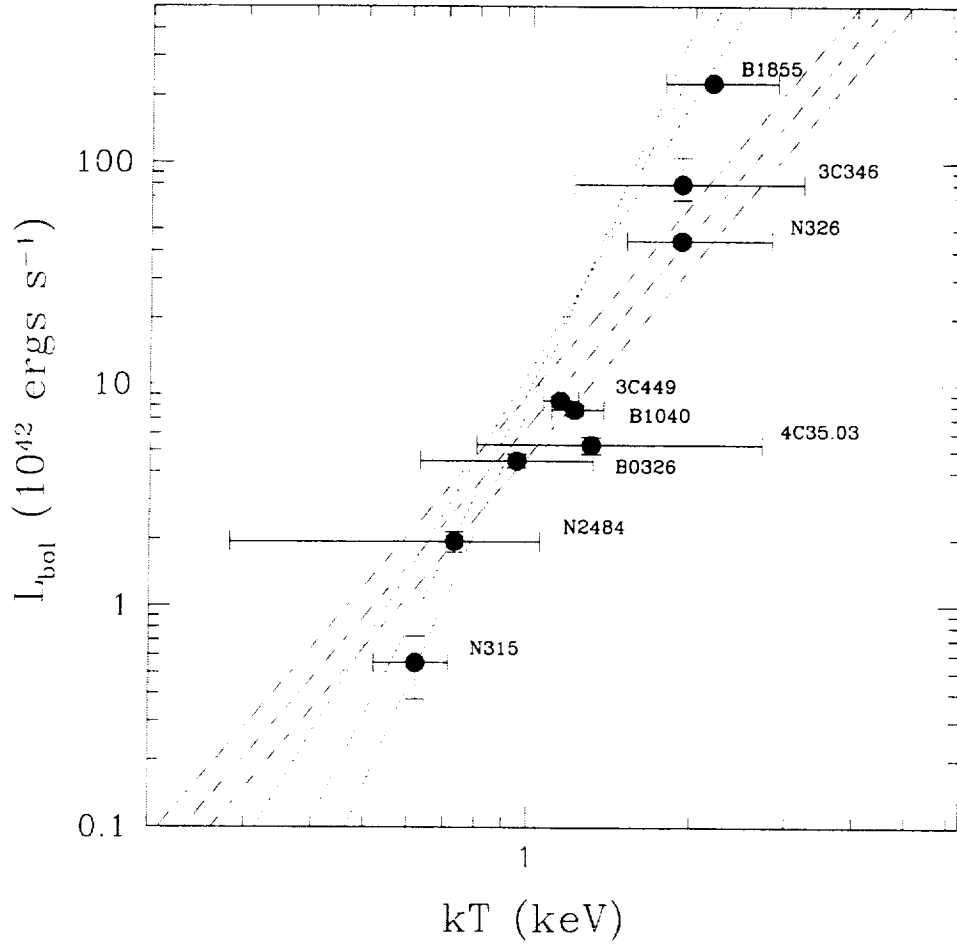


Fig. 7.— The luminosity and temperature of 3C 346's X-ray emitting atmosphere compared with results for the atmospheres of FR I radio galaxies from Worrall & Birkinshaw (2000). The dashed lines show the temperature-luminosity relation (and errors) for more luminous clusters ($\sim 10^{44} - 10^{46} \text{ ergs s}^{-1}$) from Arnaud & Evrard (1999). The dotted lines are the same for optically-selected X-ray bright groups from Helsdon & Ponman (2000), where the steeper correlation is argued to be in support of gas preheating which inhibits its collapse into the shallow potential wells of poor systems.

Table 1. X-ray Observations

Source	z	$N_{\mathrm{H}}^{\mathrm{a}}$ (cm^{-2})	Date	Mission	Instrument	Energy Band (keV)	Exposure (ks)
3C 346	0.161	5.47×10^{20}	1993 Aug 14-17	ROSAT	PSPC	0.2-2.5	16.9
			1995 Feb 17-18	ASCA	SIS, GIS	0.4-10	21.6

^aFrom Stark et al. (1992)

Table 2. Parameters for the Cluster X-ray Emission around 3C 346.

Parameter	Value
ROSAT counts (0.2-1.9 keV), $\theta < 3'$	371_{-46}^{+104}
β^{a}	$0.9_{-0.44}^{+3.1}$
$\theta_{\mathrm{cx}}^{\mathrm{a}}$	78_{-55}^{+167} arcsec
kT	$1.9_{-0.7}^{+1.3}$ keV
Density: $\theta = 0, \theta = 10''$	$1.6_{-0.4}^{+0.8} \times 10^{-3}, 1.5_{-0.3}^{+0.75} \times 10^{-3} \mathrm{cm}^{-3}$
Pressure: $\theta = 0, \theta = 10''$	$1.1_{-0.5}^{+1.0} \times 10^{-11}, 1.05_{-0.4}^{+0.9} \times 10^{-11} \mathrm{dynes cm}^{-2}$
Cooling time: $\theta = 0, \theta = 10''$	$2.6_{-1.0}^{+1.2} \times 10^{10}, 2.7_{-1.0}^{+1.2} \times 10^{10} \mathrm{years}$
$L_{0.2-2.5 \mathrm{keV}}$	$5.3_{-0.8}^{+1.6} \times 10^{43} \mathrm{ergs s}^{-1}$
$L_{0.5-3 \mathrm{keV}}$	$4.4_{-0.6}^{+1.4} \times 10^{43} \mathrm{ergs s}^{-1}$
$L_{2-10 \mathrm{keV}}$ (extrapolated)	$2_{-0.6}^{+1} \times 10^{43} \mathrm{ergs s}^{-1}$
L_{Bol} (extrapolated)	$8_{-1.2}^{+2.6} \times 10^{43} \mathrm{ergs s}^{-1}$

^a β and θ_{cx} are highly correlated and errors are for two interesting parameters. See Figure 2

Note. — All measurements are from the ROSAT PSPC observation. Errors are 1σ . Multiply pressure values by 0.1 to give in units of $\mathrm{N m}^{-2}$ (Pascals).

Table 3. Parameters for the Active Galaxy X-ray Emission in 3C 346.

Parameter	Value
ROSAT counts (0.2-1.9 keV)	736^{+21}_{-34}
ROSAT Power-law energy index, α_x	$0.69^{+0.16}_{-0.14}$
ASCA Power-law energy index, α_x	$0.73^{+0.17}_{-0.23}$
ROSAT PSPC f_1 keV	$0.162^{+0.004}_{-0.008} \mu\text{Jy}$
ASCA f_1 keV	$0.11^{+0.02}_{-0.03} \mu\text{Jy}$
ROSAT $L_{0.2-2.5}$ keV	$1.14^{+0.03}_{-0.05} \times 10^{44} \text{ ergs s}^{-1}$
ASCA $L_{0.2-2.5}$ keV (extrapolated)	$7.8^{+1.1}_{-1.7} \times 10^{43} \text{ ergs s}^{-1}$
ROSAT $L_{0.5-3}$ keV	$9.5^{+0.3}_{-0.4} \times 10^{43} \text{ ergs s}^{-1}$
ASCA $L_{0.5-3}$ keV	$6.4^{+0.8}_{-1.4} \times 10^{43} \text{ ergs s}^{-1}$
ROSAT L_{2-10} keV (extrapolated)	$1.28^{+0.04}_{-0.07} \times 10^{44} \text{ ergs s}^{-1}$
ASCA L_{2-10} keV	$8.1^{+1.2}_{-1.8} \times 10^{43} \text{ ergs s}^{-1}$

Note. — Errors are 1σ .